Transition Behaviors of Isostructural *sql*-Topological Hydrogen-Bonded Frameworks Composed of Naphthalene, Quinoxaline, and Pyrazinopyrazine Derivatives

Haruka Kubo,[a] Shunsuke Konishi,[b] Ryusei Oketani,[a] Takashi Hayashi,[b] Ichiro Hisaki*[a]

[a] H. Kubo, Dr. R. Oketani, Prof. Dr. I. Hisaki
Division of Chemistry, Graduate School of Engineering Science
Osaka University
1-3 Machikaneyama, Toyonaka, Osaka 560-8531, Japan
E-mail: i.hisaki.es@osaka-u.ac.jp

[b] S. Konishi, Prof. Dr. T. Hayashi
Department of Applied Chemistry, Graduate School of Engineering
Osaka University
2-1 Yamadaoka, Suita Osaka 565-0871, Japan

Supporting information for this article is given via a link at the end of the document.

Abstract: A series of isostructural reticular framework materials with systematic differences on chemical structures allows us to disclose correlations between specific structural factors and properties, providing insights for designing novel porous frameworks. However, even slight differences in the molecular structure often lead to non-isostructural polymorphic frameworks particularly in the case of hydrogen-bonded organic frameworks (HOFs) because the structures of HOFs are based on a subtle balance of reversible interactions. In this study, we found that three simple analogues of tetracarboxylic acids with naphthalene, quinoxaline, and pyrazinopyrazine cores (**NT**, **QX**, and **PP**, respectively) yield isostructural solvated HOFs (**NT-1**, **QX-1**, and **PP-1**, respectively), where hydrogen-bonded ***sql***-networked sheets are slip-stacked with closely similar manners, and that these HOFs undergo structural transformations in different ways by guest solvent removal. Comparison of the crystal structures of the HOFs before and after the transformation revealed that intermolecular interactions of the core significantly affected on rearrangements of hydrogen bonds after the transformation. The results suggest the potential to control the properties and functions of isostructural HOFs by elemental doping.

Introduction

A series of isostructural reticular framework materials with systematic differences on chemical and physical features is a suitable system for elucidating correlations between structures and properties of the materials.[1–3] Sophisticated isostructural porous frameworks possessing similar geometrical characteristics such as molecular arrangement or network topology[4–9] have been reported in the case of representative porous frameworks such as metal-organic frameworks (MOFs)[10,11] and covalent organic frameworks (COFs)[12], contributing to develop the strategies for designing and modulating functionality. On the other hand, hydrogen-bonded organic frameworks (HOFs)[13–17] that have garnered attention in recent years due to its high crystallinity, structural flexibility, and reusability frequently result in appearance of polymorphic frameworks. This is because HOFs are formed on the subtle balance of intermolecular interactions such as hydrogen bonding, π-π interactions, and van der Waals interactions.[18] Therefore, it is more challenging to establish a design strategy of isostructural HOFs compared to other frameworks, although developing its library for modulating structures and properties is strongly desired.

Recently, a handful of isostructural HOFs were successfully constructed by systematic modification of the arm moieties in building block molecules (tecton).[19,20] Cao, Li, and Farha independently constructed isostructural pyrene-based HOFs by introducing methyl or amino groups to the aryl arms.[21–23] Our group also reported that hexaazatriphenylene (HAT) derivatives with different length of aryl groups as the arms moieties gave four isostructural HOFs with different pore sizes.[24,25] In these cases, robust interactions orthogonally working to the hydrogen bonds, such as shape-fitted π-π stacking interactions of the cores, cooperatively work with directional hydrogen bonds of the carboxy groups, giving isostructural HOFs.

In contrast, even slight differences of the core moieties may result in diverse frameworks. For example, Li and co-workers demonstrated that 1,3,5-tris(4-carboxyphenyl)benzene and its triazine analogue possessing nitrogen atoms at 2,4,6-pisitions instead of carbon atoms formed HOFs with different interpenetration manner of H-bonded honeycomb networks although the molecular shape and geometry are closely similar with each other.[26] In these cases, introduction of iminic nitrogen atoms to the core altered the planarity of the molecules and changed the stacking patterns in the resulting frameworks. Therefore, core modifications approach remains challenging to

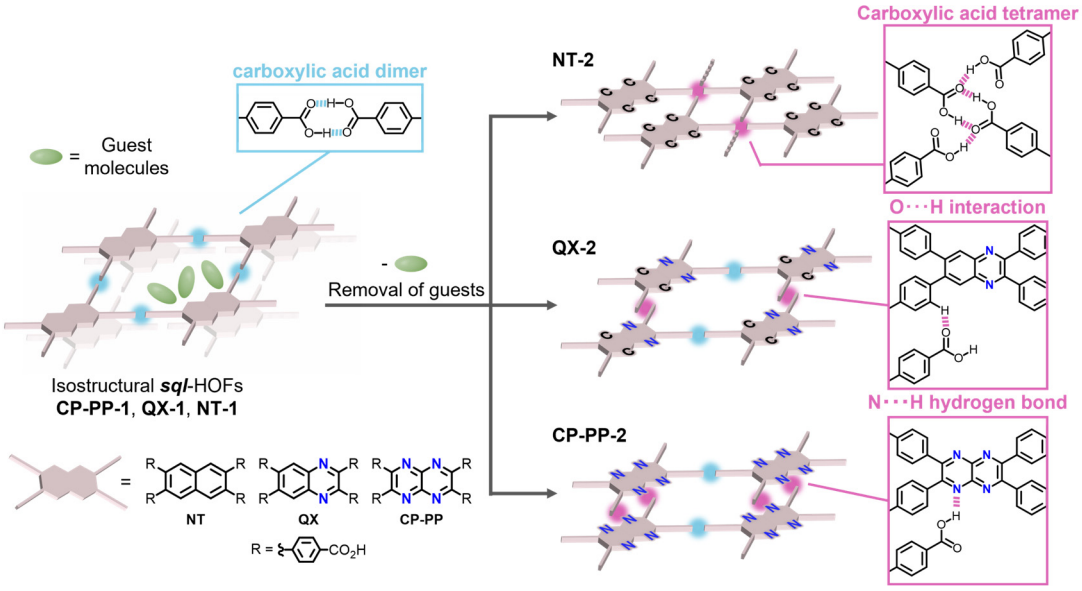

Figure 1. Overview of this study: Transformations of isostructural ***sql***-topological hydrogen-bonded organic frameworks (HOFs) composed of pyrazinopyrazine-, quinoxaline-, and naphthalene-based tetracarboxic acids **PP**, **QX**, and **NT**, respectively.

achieve isostructural HOFs, while arm modifications have been established.

To elucidate the correlation between the molecular core and structure and properties of frameworks, it is essential to construct isostructural HOFs using simpler molecular platforms with different elements as the initial trial. From this point of view, we selected tetracarboxylic acids possessing pyrazinopyrazine, quinoxaline and naphthalene cores (**PP**, **QX**, and **NT**, respectively) as a series of tectons for constructing isostructural HOFs, although HOFs of **PP** were reported in our previous work[27]. HOFs based on these molecules directly reflect the differences of the core elements on the packing structure, providing a library with different frameworks.

In this study, we crystallized **QX** and **NT** and obtained their solvated HOFs **QX-1** and **NT-1**, which are isostructural with that of previously reported HOF **PP-1** formed by **PP**, where the name, **PP-1**, is used to refer the HOF instead of previous name **CP-PP-1** due to easy recognition. These isostructural HOFs are formed through slip-stacking of ***sql***-topological H-bonded networks. Interestingly, despite having almost identical geometric features like pore size and stacking manner, these isostructural HOFs undergo structural transformations in different ways by guest solvent removal (Figure 1). Single crystalline X-ray diffraction (SCXRD) analysis on HOFs before and after the transformation revealed that intermolecular interactions of the core significantly affected on rearrangements of hydrogen bonds after the transformation, giving framework **PP-2**, **QX-2**, and **NT-2** with different H-bonding motifs. These results indicate the potential of versatile modulation of the properties and dynamic behaviors of HOFs with the initial common structural characteristics through elemental altering.

Results and Discussion

Synthesis and crystallization

Tetratopic tectons **QX** and **NT** were synthesized as shown in Scheme 1. Suzuki-Miyaura cross-coupling reaction of dimethyl 4,4'-(6,7-dibromoquinoxaline-2,3-diyl)dibenzoate (**1**)[28] and (4-(methoxycarbonyl)phenyl)boronic acid (**2**) gave ester precursor **3**. Hydrolysis of **3** in the presence of KOH yielded tetracarboxylic acid **QX**.[29] Similarly, Suzuki-Miyaura cross-coupling reaction of 3,6-dibromonaphthalene-2,7-diyl bis(trifluoromethanesulfonate) (**4**), which was synthesized according to the literature,[30] and **2** gave ester precursor **5**, which was subsequently hydrolyzed to yield **NT**. Tectons **QX** and **NT** was characterized by ^{1}H and ^{13}C NMR spectroscopy and HR-MS. Crystallization of **QX** and **NT** was conducted by slow evaporation of a mixed solution of *N,N*-dimethylformamide (DMF) and *ortho*-dichlorobenzene (DCB) at 75 °C to yield solvated HOFs **QX-1** and **NT-1** as yellow plate

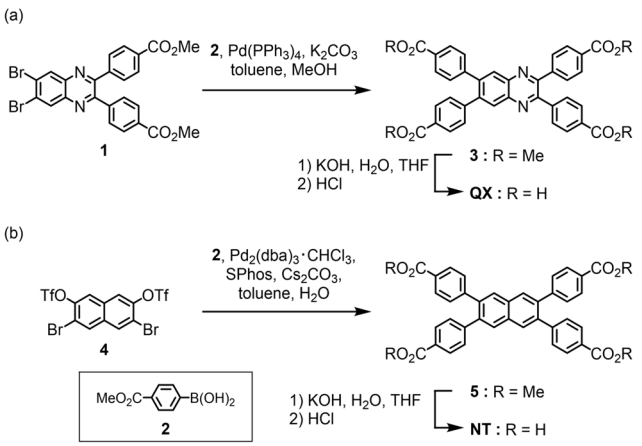

Scheme 1. Synthesis of tetracarboxylic acid building block molecules (a) **QX** and (b) **NT**.

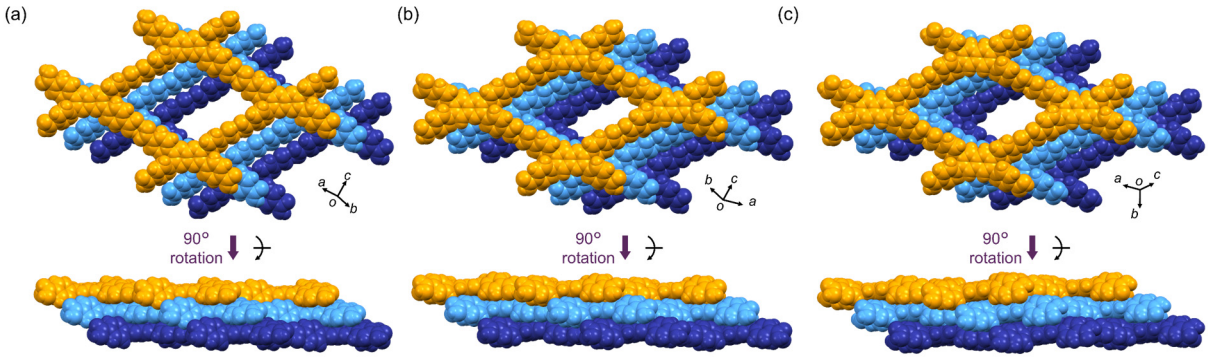

Figure 2. Overviewed crystal structures of isostructural three HOFs (a) **PP-1**, (b) **QX-1**, and (c) **NT-1**. The structure of **PP-1** was drawn using crystal data (CCDC No. 2078212) previously reported.[27]

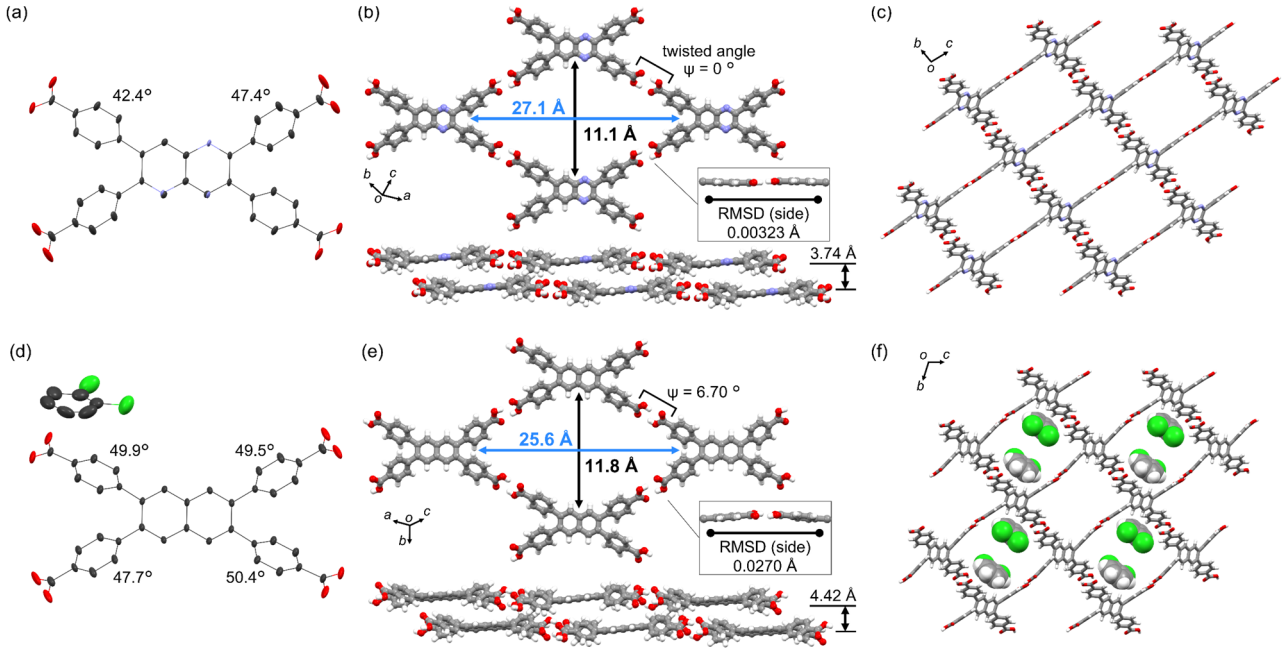

Figure 3. Crystal structures of (a-c) **QX-1** and (d-f) **NT-1**. (a, d) Molecular structure of (a) **QX** and (d) **NT** and *o*-DCB drawn with anisotropic displacement ellipsoids with 50% probability. (b, e) H-bonded rhombic network motif composed of four molecules viewed from above (top) and two layers of rhombic sheets viewed from side (bottom) in (b) **QX-1** and (e) **NT-1**. (c, f) Packing diagrams viewed from the *a* axis. The *o*-DCB molecules are included in voids, although they are not shown in the figure due to disorder in (c) **QX-1**. A part of guest molecules were capable of solving as shown in (f) **NT-1**. The atoms at positions 1, 4, 5, and 8 of the quinoxaline ring were refined with sp^2-carbon and nitrogen atoms sharing position at a 50% occupancy each, and one of sp^2-carbon and nitrogen atoms is omitted for clarity in (b) and (c).

crystals and colorless block crystals, respectively. These single crystals were subjected to SCXRD analysis.

Crystal structures of the initial solvated HOFs

Figure 2 shows overviewed crystal structures of **QX-1** and **NT-1**, together with that of previously reported **PP-1**[27] as a reference. In these crystals, the tetracarboxylic acids are connected through intermolecular H-bonds, giving a ***sql***-topological 2D network. The network structure is assemblied with a slip-stacking fashion to give isostructural frameworks, although relative orientation of the neighboring layers slightly differs from each other. The details of these crystal structure are discussed as follows.

Detailed crystal structures of **QX-1** and **NT-1** are shown in Figure 3. **QX-1** belongs to the triclinic system with space group *P*-1. Since a molecule of **QX** is disordered in the crystal, the molecule has an inversion center at the center of the quinoxaline moiety: The atoms at positions 1, 4, 5, and 8 of the quinoxaline ring were refined with sp^2-carbon and nitrogen atoms sharing position at a 50% occupancy each (Figure 3a). The twisted angles between the two independent phenylene groups and the quinoxaline core are 42.7° and 47.4°. The peripheral carboxy groups of **QX** form a dimer through self-complementary H-bonding with a O•••O distance of 2.60−2.61 Å to give a ***sql***-topological 2D networked sheet. The sheet contains rhombic voids with aperture dimension of 27.1 Å × 11.1 Å (Figure 3b). The sheets are stacked in an inclined AA pattern along the *a* axis with

an interplanar distance of 3.74 Å. CH•••π interaction are formed between the aromatic hydrogen atom of the phenylene group and benzene ring of **QX** or the phenylene group in adjacent layer (Figures S1 and S2). Additionally, there are also intermolecular H-bonding interactions such as C−H•••N interaction and C−H•••O interaction. C−H•••N interactions are formed between the N atom of **QX** and the aromatic hydrogen atom of the phenylene group with the C−H•••N distance of 2.72 Å. C−H•••O interactions are formed between the O atom of carboxylic acid and the aromatic hydrogen atom of the phenylene group in adjacent layer with the C−H•••O distance of 2.58 Å. The HOF has inclusion channels with rectangular-shaped aperture with 8.34 Å × 7.94 Å (Figure 3c). A void ratio was estimated to be 30.3% by PLATON.[31] The guest molecules exhibited significant disorder, making it difficult to determine their positions in **QX-1**.

NT-1 also belongs to the triclinic system with space group *P*-1. The twisted angles between the two independent phenylene groups and the quinoxaline core are 49.5° and 50.4° (Figure 2d). The peripheral carboxy groups of **NT** form a dimer through self-complementary H-bonding with a O•••O distance of 2.60−2.63 Å to give a ***sql***-topological 2D networked sheet. The sheet contains rhombic voids with aperture dimensions of 25.6 Å×11.8 Å (Figure 3d). The sheets are stacked in an inclined AA pattern along the *a* axis with an interplanar distance of 4.42 Å. CH•••π interaction are formed between the aromatic hydrogen atom of the phenylene group and benzene ring of **NT** or the phenylene group in adjacent layer (Figures S3 and S4). C−H•••O interactions are also formed between the O atom of carboxylic acid and the aromatic hydrogen atom of the phenylene group in adjacent layer with the C−H•••O distance of 2.56−2.61 Å. The HOF has two types of inclusion channels with rectangular-shaped aperture with 8.71 Å × 8.21 Å and 9.53 Å × 8.92 Å, respectively (Figure 3f). A void ratio was estimated to be 30.1% by PLATON. Although guest molecules were disordered, the alignment of a part of guest molecules could be determined. The *o*-DCB was inclined at 73.09° to the naphthalene ring, forming a CH-π interaction denoted by (i) in Figure 3d.

Table 1. Selected structural parameters of three HOFs **PP-1**, **QX-1**, and **NT-1**.

	PP-1	**QX-1**	**NT-1**
ω[a] / °	19.7, 55.9	42.4, 47.4	47.7, 50.4, 49.5, 49.9
Dimension of rhombic motif	13.7 Å×24.5 Å	11.1 Å×27.1 Å	11.8 Å×25.6 Å
Distance between O•••O of carboxylic acid / Å	2.62	2.60–2.61	2.60–2.63
Stacking distance / Å	3.36	3.74	4.42
Void ratio[b]	29.9%	30.3%	30.1%
ψ[c] / °	0	0	5.47, 8.44 (ave. 6.70)
RMSD (arm) [d] / Å	0.00175	0.00323	0.0270

[a] The dihedral angles of carboxyphenyl groups against the central core. [b] Solvent accessible surface. [c] The dihedral angles between H-bonded carboxyphenyl groups. [d] The root mean square deviation (RMSD) on the planes formed by H-bonded carboxyphenyl groups.

There are several subtle differences among **PP-1**, **QX-1**, and **NT-1** in terms of molecular geometry and distortions of the rhombic frameworks although they have common slip-stacked layered structures based on ***sql***-topological sheets (Table 1). The dihedral angles between the phenylene groups and the core (ω) are 19.7° and 55.9° for **PP**, whereas 42.4° and 47.4° for **QX**, and ca. 50° for **NT**. The steric hindrance of the aromatic hydrogen atoms in the core of **QX** or **NT** prevent the dihedral angle from being small. This tendency is also observed in other ***sql***-topological HOFs composed of X-shaped tetracarboxylic acids: for example, tetrakis(carboxyphenyl)benzene derivative **X-Ph**[32] exhibits the ω values of 51.1° and 52.7° in the HOF, while **X-TTF**[32,33] and **Br-PQ** [34], which lack the aromatic hydrogen atoms at the ortho positions in the core, exhibits smaller values [35.1° and 43.8° for **X-TTF**, and 21.8° and 63.4° for **Br-PQ**].

The bending of carboxylic acid dimers is observed only in **NT-1**, resulting slightly distorted rhombic network. The twist angle of the carboxylic acid dimers (ψ) is 6.7° for **NT-1** while the carboxylic acid dimers are not twisted at all in **PP-1** and **QX-1**. To evaluate distortions of the rhombic frameworks, we calculated the root mean square deviation (RMSD) on the planes formed by hydrogen-bonded carboxyphenyl groups [RMSD(arm)]. The RMSD(arm) for **NT-1** is approximately ten times larger than that for **PP-1** and **QX-1**, indicating that **NT-1** is more distorted framework compared to the other two.

Structural transformations

In the thermogravimetric (TG) and differential thermal (DT) analyses, it was observed that **PP-1**, **QX-1**, and **NT-1** showed each total weight loss of 42%, 37% and 38%, respectively, which corresponds to a host-guest ratio of 1:2 (Figure 4a,b,c). The TG curve of **PP-1** indicates *o*-DCB molecules are released in three steps. Similarly, the TG curve of **QX-1** indicates that *o*-DCB molecules are clearly released in two steps. Three-fourths of *o*-DCB molecules are released in the first step up to 156 °C. the other DCB molecules are released in the second step up to 210 °C. In contrast, the TG curve of **NT-1** has no clear plateau under 179 °C, suggesting continuous release of the solvent. Molecules of *o*-DCB began to desorb gradually at room temperature and completed desorption at 179 °C. These behaviors are strongly related to disorder of *o*-DCB molecules in the crystal structures as shown in Figure 3. In all cases of **PP-1**, **QX-1**, and **NT-1**, additional heating resulted in weight loss beyond 400 °C, corresponding the onset of decomposition.

To investigate their transition behaviors triggered by removal of solvent molecules, variable-temperature powder X-ray diffraction (VT-PXRD) patterns were recorded on as-formed crystalline bulks of solvated HOFs as heated from room temperature to 365 °C (Figure 4d,e,f). **PP-1** underwent three-step structural transformations including the first transformation from **PP-1** to **PP-2** at 105 °C followed by continuous structural changes, which is the similar behavior with thoese reported previously.[27]

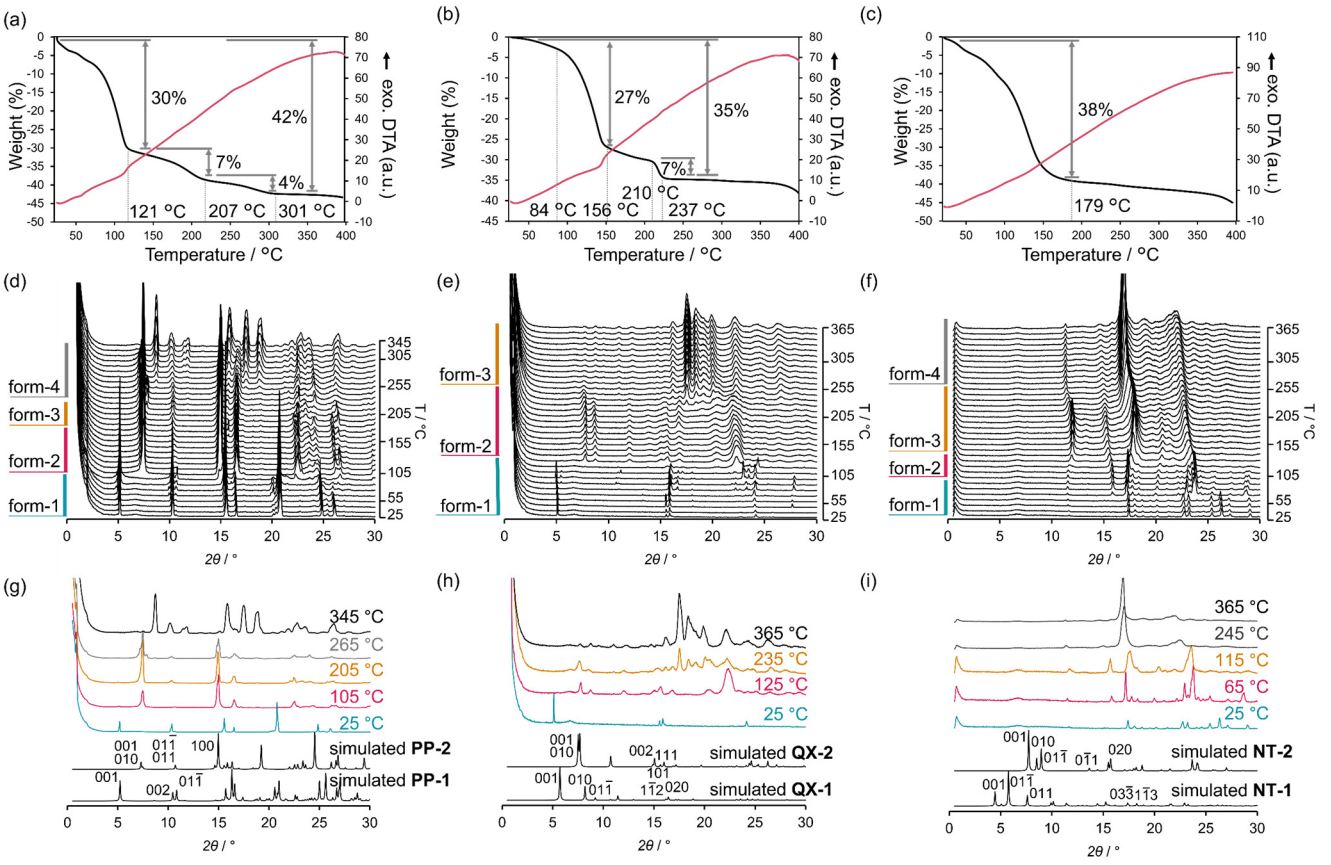

Figure 4. Thermal behaviors of (a, d, g) **CPPP-1**, (b, e, h) **QX-1**, and (c, f, i) **NT-1.** (a-c) TG-DT curves and (d-f) VT-PXRD patterns. (g-i) Representative patterns from VT-PXRD and simulated patterns from SCXRD.

QX-1 transformed to **QX-3** via **QX-2** through two-step structural changes upon heating. The peak at 2θ = 5.1° disappeared at 125 °C, and new peaks appeared at 2θ = 7.8° and 8.8°, indicating that **QX-1** transformed to **QX-2**. Further heating up to 225 °C led to the diminution of these peaks, and a new peak at 2θ = 11.1° appeared, implying that **QX-2** transformed to **QX-3**. In the case of **NT-1**, the initial form seems to transform to **NT-4** by three steps via **NT-2** and **NT-3**. The changes, however, occurred gradually, which obviously differs from non-continuous steped changes observed for **QX-1**. Transformation of **NT-1** into **NT-2** took place at a lower temperature of 65 °C compared to **QX-1**. Subsequently, in the temperature range of 115 °C to 235 °C, a gradual shift towards lower angles was observed for 2θ = 11.8 and 17.7°, indicating a continuous structural change (**NT-3**). At 245 °C, the peak at 2θ = 11.8° no longer shifted, corresponding the transition to **NT-4**. This result suggests that **PP-1** and **NT-1** exhibits similar transition behaviors, while **QX-1** transformed less readily compared to the former two, presumably due to less uniformity of the crystal provided by disorder of the quinoxaline core as well as that of the included solvent molecules.

To elucidate transformed structures, we attempted to obtain single crystals of their intermediate forms. After many efforts, we revealed that placing **QX-1** and **NT-1** under reduced pressure overnight each at 60 °C and at room temperature yielded crystals of **QX-2** and **NT-2** that partially maintain single crystallinity suitable for SCXRD analysis, although quality of crystal data of **QX-2** remains low despite our efforts. These crystal structures are shown in Figure 5. The crystal structure of **PP-2** was drawn on the basis of reported one.[27] In all cases of **PP-1**, **QX-1**, and **NT-1**, the two diagonal carboxy groups retained the H-bonded dimers, while the other two deformed H-bonded dimers were cleaved and re-bonded with different groups, resulting in different alignment of one-dimensional (1D) chain motifs.

In the case of **PP-2**, The 1D chains interact through hetero H-bonds between the carboxy group and the N atom of the **PP** core as reported.[27] In the case of **QX-2**, 1D chain of **QX** formed by H-bonding of carboxylic acid dimers with an O•••O distance of 2.63 Å are stacked in the *c*-axis direction, through π•••π and CH•••π interactions between the core and peripheral phenyl groups, resulting in a layered structure with interlayer distance of 3.62 Å (Figure 6a). On the other hand, there is no significant interactions between the 1D chains adjacent in the same plane. Only weak interactions between the carboxy oxygen atom and aromatic hydrogen atoms are suggested. Disordered solvent molecules may also support this packing structure. The twist angles between the peripheral phenyl groups and the core plane are 28.6° and 60.8°, which are smaller than the dimer formation angles of the carboxylic phenyl groups in **QX-1** (42.7° and 47.4°). The sheet contains rhombic voids with aperture dimension of 16.2 Å × 12.9 Å. The void ratio was estimated to be 8.2%.

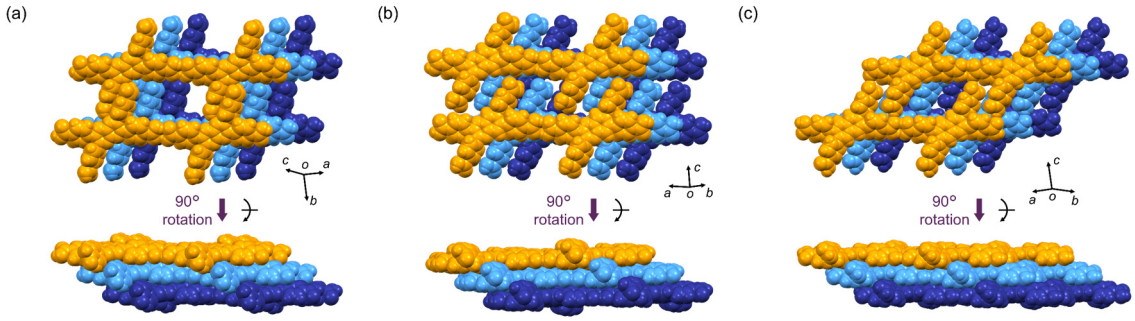

Figure 5. Overviews of three transformed HOFs (a) **PP-2**, (b) **QX-2**, and (c) **NT-2**. The structure of **PP-2** was drawn using crystal data (CCDC No. 2080627) previously reported [27].

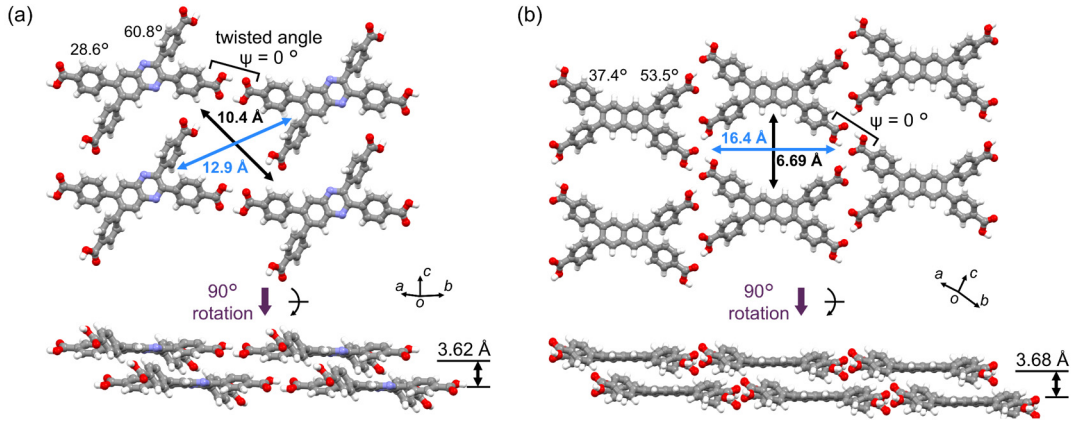

Figure 6. (a) H-bonded 1D chain motifs viewed from above (top) and two layers of sheets viewed from side (bottom) in **QX-2**. The atoms at positions 1, 4, 5, and 8 of the quinoxaline ring were refined with sp^2-carbon and nitrogen atoms sharing position at a 50% occupancy each. One of sp^2-carbon and nitrogen atoms is omitted for clarity in (a). (b) Hydrogen-bonded 2D chain network motif viewed from above (top) and two layers of sheets viewed from side (bottom) in **NT-2**. The *o*-DCB are included in voids, although they are not shown in the figure due to disorder in both of (a) **QX-2** and in (b) **NT-2**.

NT formed cross-shaped carboxylic acid tetramer by combination of the carboxylic acid dimer and other two carboxy groups (Figure 6b). This H-bonding motif is also observed in other HOFs, such as **PFC-79**[33] based on a tetrathiafulvalene tetracarboxylic acid derivative and **BrPQ-2**,[34] based on a dibromopyrazinoquinoxaline tetracarboxylic acid derivative. The O•••O distance of the carboxyl dimers is 2.64 Å, and that in the branched H-bonds is 2.67 Å. Similar to **QX-2**, stacking was achieved through π•••π interactions between the core and peripheral phenyl groups or CH•••π interactions, resulting in a layered structure with interlayer distance of 3.68 Å. The twist angles of the peripheral phenyl groups to the core plane are 37.4° and 53.5°, smaller than the dimer formation angles of the carboxylic phenyl groups in **NT-1** (49.5° and 50.4°). The sheet has a rhombic void with small aperture dimension of 16.4 Å × 6.69 Å. The void ratio was estimated to be 5.7%.

H-bonding interactions between the 1D chain motifs were calculated. In the case of **PP-2**, hetero H-bonds between the carboxy group and nitrogen atom in the PP cores are estimated to be −51.3 kJ/mol (Figure S5, Tables S2–S6). A weak C-H•••O H-bond between the carbonyl and phenylene groups in **PP-2** has a binding energy of −10.9 kJ/mol. In the case of **QX-2**, only C-H•••O interactions was observed between the carbonyl and phenylene groups with an interaction energy of −12.0 kJ/mol (Figure S6, Tables S7–S10). A blanched H-bond observed in **NT-2** exhibits an interaction energy of 38.5 kJ/mol (Figure S7, Tables S11–S13). Thus, H-bonds working between the 1D chain motifs are larger in the order of **QX-2**, **NT-2**, and **PP-2**.

Compared to PXRD patterns simulated from crystal structures, PXRD patterns of **QX-2** observed at 125 °C match simulated patterns although observed patterns included other peaks. Through this comparison, the crystalline bulk of **QX-2** seemed to contain several polymorphic crystal structures. Solving the crystal structure using a PXRD pattern of **NT-2** was hard because intensity of PXRD peaks in the small angle region was too weak for indexing. However, we obtained the crystal structure of one of the phases undergoing continuous change by SCXRD. Attempts were also made to reveal crystal structures of **QX-3**, **NT-3**, and **NT-4** by SCXRD analyses on solid samples obtained by further heating, resulting failure due to significant decrease in crystallinity. However, the solvent free forms **QX-3** and **NT-3** showed permanent porosity with small Brunauer-Emmett-Teller (BET) surface areas of 49 $m^2\ g^{-1}$ and 288 $m^2\ g^{-1}$, respectively (Figures S8–S11).

Conclusion

We constructed novel HOFs, **QX-1** and **NT-1**, consisting of tetracarboxylic acids with systematically modified naphthalene skeletons with iminic nitrogen atoms, and explored the structures and properties of three isostructural HOFs **PP-1**, **QX-1**, and **NT-1** to elucidate the effects of the nitrogen atoms into the core. SCXRD analysis revealed that the frameworks of the three HOFs were geometrically similar, i.e. isostructures. Their thermal behaviors showed that **PP-1**, **QX-1** and **NT-1** underwent structural transitions into **PP-2**, **QX-2** and **NT-2**, respectively, accompanied by guest removal trigered reconstruction of intermolecular H-bonds. **PP-2** contains hetero H-bonds between iminic nitrogen and carboxylic hydrogen. **QX-2** contains weak CH•••O interactions. **NT-2** contains blanched H-bonds of carboxylic acid tetramers. The presence of imine nitrogen in the core provided stabilization through N•••H hydrogen bond formation, while the sp^2 carbon perticilates in weak CH•••π interactions. These results contribute to establishing guidelines for controlling transition behavior without altering the initial framework structure.

Supporting Information

The authors have cited additional references within the Supporting Information.[35-49] Synthetic procedure, experimental details, detailed intemolecular interactions, gas sorption isotherms, theoretical calculations, NMR spectra of the synthesized compounds (PDF), and crystal structures of **QX-1** (CIF), **NT-1** (CIF), **QX-2** (CIF), **NT-2** (CIF). CCDC 2350221-2350224 contain the supplementary crystallographic data for this paper. These data can be obtained free of charge via www.ccdc.cam.ac.uk/data_request/cif, or by emailing data_request@ccdc.cam.ac.uk, or by contacting The Cambridge Crystallographic Data Centre, 12 Union Road, Cambridge CB2 1EZ, UK; fax: +44 1223 336033.

Acknowledgements

This work was supported by KAKENHI (JP21H01919, JP22H05461, JP23H04029, and JP24K01468) from JSPS and MEXT Japan. H. K. thanks finantial support by JST, the establishment of university fellowships towards the creation of science technology innovation (JPMJFS2125). I. H. thanks Hoansha Foundation and the Multidisciplinary Research Laboratory System for Future Developments (MRL), Graduate School of Engineering Science, Osaka University for their finantial support. The authors thank the Cybermedia Center, Osaka University, for use of the Super-computer for Quest to Unsolved Interdisciplinary Datascience (SQUID). The authors acknowledge Prof. Dr. N. Tohnai and M. Naruoka at Osaka University for gas sorption experiments and Ms. R. Miyake at Osaka University for HR-MS analysis.

Keywords: hydrogen-bonded framework • isostructure • flexibility • porous molecular crystal • crystal engineering

[1] H. Deng, C. J. Doonan, H. Furukawa, R. B. Ferreira, J. Towne, C. B. Knobler, B. Wang, O. M. Yaghi, *Science* **2010**, *327*, 846–850.
[2] L. Feng, K. Y. Wang, G. S. Day, H. C. Zhou, *Chem Soc Rev* **2019**, *48*, 4823–4853.
[3] C. S. Diercks, O. M. Yaghi, *Science* **2017**, *355*,.aal1585.
[4] A. G. Slater, A. I. Cooper, *Science* **2015**, *348*, aaa8075.
[5] C. S. Diercks, Y. Liu, K. E. Cordova, O. M. Yaghi, *Nat Mater* **2018**, *17*, 301–307.
[6] M. J. Kalmutzki, N. Hanikel, O. M. Yaghi, *Sci. Adv.* **2018**, *4*, eaat9180.
[7] C. Gropp, S. Canossa, S. Wuttke, F. Gándara, Q. Li, L. Gagliardi, O. M. Yaghi, *ACS Cent Sci* **2020**, *6*, 1255–1273.
[8] Y. B. Zhang, Q. Li, H. Deng, *Nano Res* **2021**, *14*, 335–337.
[9] W. Xu, B. Tu, Q. Liu, Y. Shu, C. C. Liang, C. S. Diercks, O. M. Yaghi, Y. B. Zhang, H. Deng, Q. Li, *Nat Rev Mater* **2020**, *5*, 764–779.
[10] O. Yaghi, G. Li, H. Li, *Nature* **1995**, *378*, 703–706.
[11] M. Kondo, T. Yoshitomi, K. Seki, H. Matsuzaka, S. Kitagawa, *Angewandte Chemie* **1997**, *109*, 1844–1846.
[12] Adrien P. Coˆte´, Annabelle I. Benin, Nathan W. Ockwig, Michael O'Keeffe, Adam J. Matzger, Omar M. Yaghi, *Science* **2005**, *310*, 1164–1166.
[13] K. Endo, T. Sawaki, M. Koyanagi, K. Kobayashi, Y. Aoyama, K. Endo, Y. Aoyama, H. Masuda, *J Am Chem Soc* **1995**, *117*, 8341–8352.
[14] P. Sozzani, A. Comotti, R. Simonutti, T. Meersmann, J. W. Logan, A. Pines, *Angewandte Chemie - International Edition* **2000**, *39*, 2695–2699.
[15] Y. He, S. Xiang, B. Chen, *J Am Chem Soc* **2011**, *133*, 14570–14573.
[16] I. Hisaki, C. Xin, K. Takahashi, T. Nakamura, *Angewandte Chemie - International Edition* **2019**, *58*, 11160–11170.
[17] R. B. Lin, Y. He, P. Li, H. Wang, W. Zhou, B. Chen, *Chem Soc Rev* **2019**, *48*, 1362–1389.
[18] H. Wang, Z. Bao, H. Wu, R. B. Lin, W. Zhou, T. L. Hu, B. Li, J. C. G. Zhao, B. Chen, *Chemical Communications* **2017**, *53*, 11150–11153.
[19] A. Pulido, L. Chen, T. Kaczorowski, D. Holden, M. A. Little, S. Y. Chong, B. J. Slater, D. P. McMahon, B. Bonillo, C. J. Stackhouse, A. Stephenson, C. M. Kane, R. Clowes, T. Hasell, A. I. Cooper, G. M. Day, *Nature* **2017**, *543*, 657–664.
[20] M. I. Hashim, H. T. M. Le, T. H. Chen, Y. S. Chen, O. Daugulis, C. W. Hsu, A. J. Jacobson, W. Kaveevivitchai, X. Liang, T. Makarenko, O. Miljanić, I. Popovs, H. V. Tran, X. Wang, C. H. Wu, J. I. Wu, *J Am Chem Soc* **2018**, *140*, 6014–6026.
[21] F. Hu, C. Liu, M. Wu, J. Pang, F. Jiang, D. Yuan, M. Hong, *Angewandte Chemie* **2017**, *129*, 2133–2136.
[22] Q. Yin, P. Zhao, R.-J. Sa, G.-C. Chen, J. Lü, T.-F. Liu, R. Cao, *Angewandte Chemie* **2018**, *130*, 7817–7822.
[23] Y. Wang, K. Ma, J. Bai, T. Xu, W. Han, C. Wang, Z. Chen, K. O. Kirlikovali, P. Li, J. Xiao, O. K. Farha, *Angewandte Chemie - International Edition* **2022**, *61*, DOI 10.1002/anie.202115956.
[24] Y. Suzuki, M. Gutiérrez, S. Tanaka, E. Gomez, N. Tohnai, N. Yasuda, N. Matubayasi, A. Douhal, I. Hisaki, *Chem Sci* **2021**, *12*, 9607–9618.
[25] Y. Suzuki, M. Yamaguchi, R. Oketani, I. Hisaki, *Mater Chem Front* **2022**, *7*, 106–116.
[26] Y. L. Li, E. V. Alexandrov, Q. Yin, L. Li, Z. Bin Fang, W. Yuan, D. M. Proserpio, T. F. Liu, *J Am Chem Soc* **2020**, *142*, 7218–7224.
[27] Q. Ji, K. Takahashi, S. I. Noro, Y. Ishigaki, K. Kokado, T. Nakamura, I. Hisaki, *Cryst Growth Des* **2021**, *21*, 4656–4664.
[28] A. V. Yagodin, I. A. Mikheev, D. A. Bunin, A. A. Sinelshchikova, A. G. Martynov, Y. G. Gorbunova, A. Y. Tsivadze, *Dyes and Pigments* **2023**, *216*, DOI 10.1016/j.dyepig.2023.111326.
[29] S. Mi, L. Wang, H. Guo, Y. Su, S. Wang, J. Xu, J. Cao, X. Guo, *Cryst Growth Des* **2024**, *24*, 405–413.
[30] Y. Li, X. Su, W. Zheng, J. J. Zheng, L. Guo, M. Bonn, X. Gao, H. I. Wang, L. Chen, *Angewandte Chemie - International Edition* **2023**, *62*, DOI 10.1002/anie.202216795.
[31] A. L. Spek, *Acta Cryst.* **2009**, *D: Biol. Crystallogr*, 148–155.
[32] I. Hisaki, N. Q. Emilya Affendy, N. Tohnai, *CrystEngComm* **2017**, *19*, 4892–4898.
[33] X. Y. Gao, Y. L. Li, T. F. Liu, X. S. Huang, R. Cao, *CrystEngComm* **2021**, *23*, 4743–4747.
[34] H. Kubo, R. Oketani, I. Hisaki, *Chemical Communications* **2021**, *57*, 8568–8571.